Contents

Chapter 1

Reconstruction of Physics Object

ATLAS raw data, which stores the detectors signals of all the read-out channels, are rather inconvenient for data analysis. Typically, those data undergo to several steps of reconstruction before being ready for the analyzers use. Reconstruction software is hold within the ATLAS reconstruction software framework ATHENA [47]. In this framework, physics observables reconstruction and particle identification are performed in an object orient fashion.

This chapter briefly describes the ATLAS strategies for physics object reconstruction used in chapter **??**. For a detailed overview of the ATLAS detector reconstruction software see [48].

1.1 Tracks Reconstruction

The reconstruction of charged particles tracks and interaction vertex is based on Inner Detector information, which allows tracks reconstruction within $|\eta| < 2.5$. Charged particle bends in the transverse plane due to the magnetic field of the Inner Detector and transverse momentum measure can be achieved. A track is characterized by its momentum vector and two *impact parameters*: d_0, which is the distance of closest approach of the track to the interaction point in the $x - y$ projection and z_0, which is the z coordinate of the track calculated at the same point.

Tracks are reconstructed by the Inner Detector track reconstruction software [49]. First raw data from the pixel and SCT detectors are transformed in three dimensional space points which are called "hits", while the TRT detector information is translated into drift circles. Then, track seeds are formed from a combination of space-points in the three pixel layers and the first SCT layer, these seeds are then extended throughout the SCT to form track candidates. The tracks candidate are fitted using a *Kalman filter* algorithm [50], ambiguities in the cluster-to-track association are resolved and fake tracks are rejected. The selected tracks are then extended to the TRT and finally refitted with the full information of all three detectors. To help improve tracking efficiency for secondary tracks coming from photon conversion or decays of long-lived particles (like kaons), a complementary algorithm searches for unused track segments in the TRT, which will be then extended towards the SCT and the pixel in a very similar way as described for the default algorithm. All tracks found with $P_T > 100$ MeV are written to the database.

1.2 Vertex Reconstruction

The vertex reconstruction algorithm and its performance are described in full detail in [48, 51] and only briefly summarized here. The vertex finding is performed as follows: a set of well reconstructed tracks are selected, a vertex is seeded according to the global maximum of the selected tracks z coordinate distribution, the tracks z coordinate is computed with respect the expected average collision point. An *adaptive vertex fitting* algorithm [52] determines the vertex position taking as input the vertex seed position and the tracks around it. Tracks that are incompatible with the found vertex by more than seven standard deviation are used to seed the next vertex. The iteration continues until no tracks are left or no additional vertex can be found. The procedure depends on the expected position of the average interaction point, which is monitored during LHC data taking and is computed every few minutes with the method described in [53].

The vertex with the larger sum of tracks P_T associated is identified as the *primary vertex* (PV), which is the interaction point related to the hard scattering of the event. All the other vertices are assumed to result from minimum bias interaction and are called *pile-up* vertices. In data recorded during 2012, an average of 21 multiple interaction are occurred per bunch crossing, such a high vertex multiplicity strongly affects the ambient energy density in the event, a correct pile-up description is then crucial for MC simulation. In ATLAS, simulated events are produced under various pile-up conditions, the events are then weighted according to the average interaction per bunch crossing recorded in data.

1.3 Electrons Reconstruction

Electron are reconstructed combining EM calorimeter and Inner Detector information, the ATLAS dedicated electron reconstruction algorithm is presented in [54]. The electron reconstruction starts from clusters of EM calorimeter cells, tracks are sought in the Inner Detector to match the clusters, special care is taken in order to account for Bremsstrahlung losses during the track matching stage. An electron candidate is defined as a cluster in the EM calorimeter combined with a track. The electron energy is computed as a weighted average between the cluster energy and the track momentum, several corrections are applied to take into account energy loss in the material of the Inner Detector and effect of electromagnetic shower leakage. The electron direction is taken from the corresponding track parameters.

Further selection are applied to the electron candidates to reduce contamination from photon conversion and hadronic jet, three different identification criteria are provided:

- Loose: selections related to the shape of the shower and to hadronic leakage are applied.
- Medium: additionally to the loose requirements, information on the strip layer of the electromagnetic calorimeter is used, stricter track matching requirements are also applied.
- Tight: additionally to medium requirements, converted photons are rejected by requiring a hit in the Inner Detector b-layer (if the module is expected to be operating), TRT electron identification capability is employed.

The electron identification performances are compared between data and simulation in [55], correction to the electron identification efficiency are estimated and applied as weight to simulated electron candidates. Additional corrections are applied to the energy scale and resolution of simulated electron to match the one in

data according to [56]. Finally, the electrons used in the presented analysis are rejected if matching with a region of the calorimeter with readout problems or suffering from high noise.

Prompt electrons, coming from the decay of a resonance like the Z^0 boson or the Higgs boson are very likely to be *isolated*, i.e. very little activity is expected in their surroundings, this is in contrast to electron that come from decay of hadrons, which instead will be likely to be embedded in a jet of particle. Two isolation variables are then defined by the sum of the energy in a $\Delta R = \sqrt{\Delta\phi^2 + \Delta\eta^2}$ cone around the electron candidate:

- Track isolation P_T^{cone}: which is the scalar sum of the track P_T in a $\Delta R \leq 0.4$ cone around the electron, the electron track is not considered.
- Calorimeter isolation E_T^{cone}: which is the scalar sum of topological cluster transverse energy in a $\Delta R \leq 0.2$ cone around the electron. Cluster associated to the electron are not considered. This variable is corrected as a function of the vertex multiplicity in the event in order to assure a constant selection efficiency.

1.4 Muons Reconstruction

ATLAS employs a variety of strategies for identifying and reconstructing muons, the main detector used for this purpose is the Muon Spectrometer, which may be supplemented with others detectors informations. A detailed description of the muon reconstruction algorithms and their performance is reported in [48], in the following only the muon reconstruction strategy relevant for this thesis is described.

The STACO *combined* muon algorithm [57] associate tracks found in the Muon Spectrometer with the corresponding Inner Detector track and calorimeter information, the muons are then identified at their production vertex with optimum parameter resolution. First track segment are reconstructed in each of the three muon station, segments are then liked together to form a track. The muon track is extrapolated to the Inner Detector taking into account energy loss and multiple scattering in the calorimeters, then, it is matched with a Inner Detector track via χ^2 matching. Finally a statistical combination of the Inner Detector and Muon Spectrometer tracks is performed to obtain a combined vector.

Muon reconstruction efficiency, momentum scale and resolution are evaluated in [58], performance are compared with MC simulation and a set of corrections, aimed to restore agreement between data and simulation, are provided. Correction on muon momentum scale, resolution and reconstruction efficiency are applied to muons in the presented analysis.

Isolation variable, as described for electrons, are also implemented for muons, the only exception is the use of calorimeter cluster with fixed size (towers) in the definition of E_T^{cone}. Similar pile-up corrections are also used for muons.

1.5 Jets Reconstruction and Energy Calibration

Jets are reconstructed in ATLAS by means of the FastJet package [59], which provides a broad range of jet finding algorithms and analysis tools. In the following jet reconstruction methods relevant for the analysis presented in this theses are briefly described, for more detail see [48].

In general, jets may be reconstructed out of any set of four vector objects, however in ATLAS, the most important detectors for jet reconstruction are the ATLAS calorimeters. Calorimeter cells are grouped together by a clustering algorithm forming what are called *topological clusters* [60], those are three-dimensional cluster representing the energy deposition of the shower. the clustering starts with seed cells with a signal-to-noise ratio greater that a certain threshold, all nearby cells are grouped to the seed cells if they passes a second, lower, signal-to-noise ratio threshold.

Topological clusters are then fed to an *anti-k_t* algorithm [61]. The algorithm defines a metric to assess distances between the clusters i and j, the metric is defined as follows:

$$d_{ij} = \min(\frac{1}{k_{t,i}^2}, \frac{1}{k_{t,j}^2}) \cdot \frac{\Delta R_{ij}^2}{R^2} \tag{1.1}$$

$$d_i = \frac{1}{k_{t,i}^2} \tag{1.2}$$

where $k_{t,i}$ is the P_T of the cluster i and $\Delta R_{ij}^2 = \sqrt{\Delta\phi_{ij}^2 + \Delta\eta_{ij}^2}$. For the presented analysis $R = 0.4$ is chosen. If the distance between two cluster d_{ij} is smaller that d_i the clusters are grouped together and their four momentum summed, otherwise their are kept as single entity. The clustering procedure is iterated until no cluster can be further merged. The metric is designed in a way that high P_T clusters will accumulate the soft activity surrounding them leading to conical jet shapes.

Given the high pile-up environment of LHC is important to distinguish jets coming from the hard scattering process and those related to pile-up interaction, for this purpose, a technique called *jet vertex fraction* (JVF) is implemented in the ATLAS jet reconstruction software. The JVF relies on Inner Detector informations, it is defined as the P_T weighted fraction of tracks pointing to to the primary vertex

associated to the jet:

$$\mathrm{JVF} = \frac{\sum_{PV-tracks} P_T}{\sum_{tracks} P_T} \tag{1.3}$$

the jet vertex fraction is only available within Inner Detector coverage $|\eta| < 2.5$, while calorimeter jet reconstruction is possible up to $|\eta| < 4.5$.

Calorimeter Jet Energy Calibration The ATLAS calorimeters were calibrated using test beam electrons [62], however the response to electromagnetic shower is different from the one to hadronic shower. A dedicated jet energy scale (JES) calibration is then performed by means of MC simulation [63]: jet energy is corrected to correspond, as a mean value, to the simulated energy of the hadronizing parton origin of the jet. The direction of the jet is also corrected to constraint it to point to the primary vertex instead to the center of the ATLAS detector. A set of corrections are then evaluated to take into account effect of pile-up [64, 65]. Jet resolution is also corrected in MC to better describe the data [66]. Finally, several jet energy scale correction are applied for a better agreement between data and simulation, those corrections are evaluated based on 2011 ATLAS data and exploits several techniques, JES systematic uncertainty due not perfect MC modeling are also evaluated, a full description of JES "in-situ" methodology corrections and related systematics uncertainties are described in [63, 67].

1.6 Jet b-Tagging

The typical decay length of b-hadron at ATLAS is of the order of few millimeter. Exploiting the high precision of the Inner Detector tracker is possible to identify jet originating from b-quarks with respect to other flavors, those jets are called *b-jets* and the identification technique used *b-tagging*.

Several algorithm has been developed in ATLAS for jet b-tagging, the relevant b-tagging algorithm to this thesis are briefly described in what follows, for more detailed description see [48]. The first step of jet b-tagging is to associate tracks to jets based on a ΔR cone matching, those tracks should satisfy strict selection criteria aimed to assure good quality and to reject tracks likely to come from strange hadron decays or photon conversion. For the discrimination between b-jet and light-jet (and in some cases also c-jet) algorithms uses the MC prediction of the distribution of some discriminating variable for the two hypothesis. Given the relatively high mass of b-hadrons, the tracks associated with b-jet will have spreaded impact parameters, this feature is used by the IP3D b-jet tagging algorithm, where a discriminating variable is implemented based on the impact parameter significances

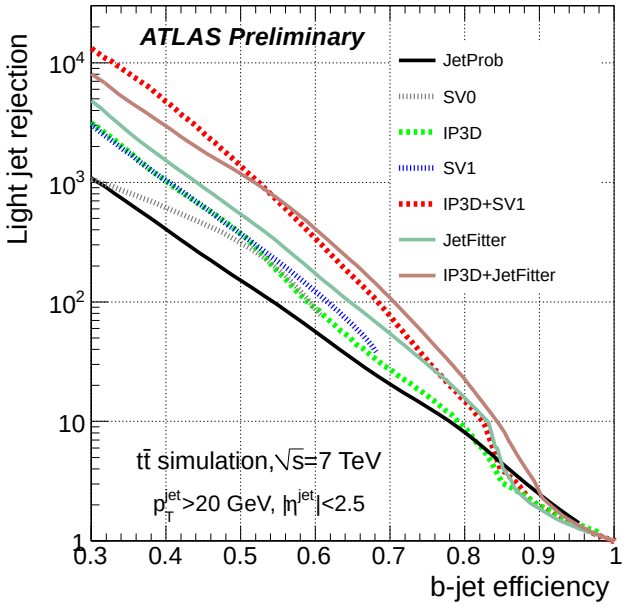

Figure 1.1: Light-jet rejection as a function of the b-jet tagging efficiency for different tagging algorithms [70]. Rejection here is defined as the inverse of mistagging rate, and the distributions are referred to a $t\bar{t}$ sample.

of the tracks associated to the jet. An alternative approach, used by the $SV1$ algorithm, is instead to searches for inclusive secondary vertex formed by the decay products of the b-hadron, the search includes also the subsequent charm hadron decays. Another algorithm, called JetFitter [69], uses instead the direction of the jet to fully reconstruct the decay chain of b-hadron, the assumption made is that the decayed particles will lie along the jet axis. Finally, the three algorithm just described are combined together using an artificial neural network to maximize the discriminating power, the output of this neural network is referred as $MV1$ and is used in the search presented in this thesis.

The performance of the mentioned algorithms are evaluated in data and compared to simulation in [70]. B-hadron tagging efficiency and mistagging rate are the most common feature that describes the performance of a b-tagging algorithm, Figure 1.1 shows the b-tagging efficiency as a function of the inverse of the mistagging rate for different b-tagging algorithm, the tagging efficiency $\epsilon_b^{t\bar{t}}$ is usually referred to b-hadron in $t\bar{t}$ events and totally specify a b-tagging selection point. Correction due to non perfect modeling of b-tagging performance are evaluated by means of several methods for 2012 data in [71, 72] and used as event weights in MC simulation.

1.7 Missing Transverse Energy

The missing transverse energy, E_T^{miss}, is the absolute value of the vectorial sum of the transverse momenta in the event. Undetected particles, such as neutrinos leads to an unbalance of the total transverse momentum, thus, to a non zero E_T^{miss}.

Reconstruction and calibration of E_T^{miss} at ATLAS is described in detail in [73]. The missing transverse energy relies on the reconstruction of all physics object in the event: it includes muons and their energy deposit in the calorimeter, electron, jets (weighted by their JVF), Inner Detector tracks (to take into account low-P_T particles not well reconstructed in the calorimeters), photons and τ leptons. The calorimeters cells are then calibrated depending on the object they are associated with. Cells not associated to any object are included in the so called "CellOut term", this term, together with the one related to jets with $10 < P_T < 20$ GeV are referred to as the *soft term* of the missing transverse energy. The soft term is found to be very sensitive to pile-up, a solution to reduce this effect is to scale it by its soft-term-vertex-fraction (STVF), which is calculated exactly as for JVF in jets.

A description of the performance of the ATLAS E_T^{miss} reconstruction and calibration may be found in [74].

1.8 Tau Hadronic Decay

The reconstruction of hadronically decaying τ candidates (in the following τ_h) is described in detail in [48]. A τ_h candidate is seeded by reconstructed calorimeter jets with $P_T > 10$ GeV and $|\eta| < 2.5$, tracks are then associated to the jet and a combination between tracking and calorimeters informations is performed. Hadronic tau decays can be distinguished from jets by their low track multiplicity and narrow clustering of electromagnetic and hadronic calorimeter activity. The τ_h identification in ATLAS is performed by a multivariate discriminant based on Boosted Decision Trees (BDTs) [75]. One BDT discriminant has been developed to discriminate τ_h from quark and gluon initiated jets and a separate BDT was developed to reject electrons. The analysis presented in the next chapter requires one or three charged tracks associated to the τ_h candidate, for the identification a "Medium" BDT working point is chosen, additionally, a BDT-based electron veto is applied.

1.9 Overlap Removal

Reconstruction of the physics object defined in the previous section may sometimes be ambiguous, for example, an hadronic τ is always reconstructed also as a jet. To avoid double counting of the same physics object a procedure of overlap removal is performed in the presented analysis. Physics object of different sort are matched in a cone of $\Delta R < 0.2$, if matching occurs, the object with the lowest ranking is removed from the event. Physics object are ranked according to the following order: first muon, then electron, hadronic τ and finally jets.

1.10 Trigger

The ATLAS trigger system [76] consists of three stages. The Level-1 (L1) trigger is a hardware trigger which reduces the event rate to approximatively 100 kHz and selects the Regions of Interest (RoI) to be further investigated by the High Level Trigger (HLT). The HLT comprises the Level-2 (L2) trigger employing fast reconstruction algorithms and the Event Filter (EF) exploiting the full ATLAS event reconstruction.

In the presented search two triggers are employed: an electron EF trigger, which selects data presenting an electron with $P_T > 24$ GeV and a combined muon-electron EF trigger, which requires a muon with $P_T > 8$ GeV and an electron with $P_T > 12$ GeV. Detailed description of the muon and electron triggers can be found in [77, 78]. Trigger efficiency for both triggers is evaluated and compared with MC prediction, corrections as function of lepton direction and momentum are derived to match MC trigger efficiency to data [77, 78], those corrections are applied in the presented analysis.

1.11 Truth Particles

In case of a simulated event, the ATLAS reconstruction software provides information regarding simulated particles (also called *truth-particles*), their identity, properties, decays and interactions are stored in the event based on the conventions defined in [79]. A particle is defined stable if $c\tau > 1$ m, where τ is its mean life time, particle emerging from interaction with the detector are excluded from this definition. Each particle has an associated "barcode" which is a unique identifier for that particle in that event. Jets reconstructed from stable particles are called *truth-jets*.

Bibliography

[1] L. Evans and P. Bryant, *LHC Machine*, JINST **3** (2008) S08001.

[2] F. Englert and R. Brout, *Broken Symmetry and the Mass of Gauge Vector Mesons*, Phys. Rev. Lett. **13** (1964) 321.

[3] P. W. Higgs, *Broken symmetries, massless particles and gauge fields*, Phys. Lett. **12** (1964) 132.

[4] P. W. Higgs, *Broken Symmetries and the Masses of Gauge Bosons*, Phys. Rev. Lett. **13** (1964) 508.

[5] P. W. Higgs, *Spontaneous Symmetry Breakdown without Massless Bosons*, Phys. Rev. **145** (1966) 1156.

[6] G. S. Guralnik, C.R. Hagen and T. W. B. Kibble Phys.Rev.Lett. **13** (1964) 585.

[7] N. P. Nilles, *Supersymmetry, supergravity and particle physics*, Phys. Rep. **110** (1984) 1.

[8] H. E. Haber and G. L. Kane, *The search for supersymmetry: Probing physics beyond the standard model*, Phys. Rep. **117** (1985) 75.

[9] ALEPH, DELPHI, L3 and OPAL Collaboration, *Search for neutral MSSM Higgs bosons at LEP*, Eur. Phys. J. **C47** (2006) 547.

[10] *Combined CDF and D0 upper limits on MSSM Higgs boson production in tau-tau final states with up to 2.2 fb^{-1} of data*, `arXiv:1003.3363 [hep-ex]`.

[11] CDF Collaboration, T. Aaltonen et al. Phys. Rev. Lett. **103** (2009) 201801.

[12] D0 Collaboration, V. Abazov et al. Phys. Rev. Lett. **101** (2008) 071804.

[13] TNPWG (Tevatron New Physics Higgs Working Group), CDF and D0 Collaborations, *Search for Neutral Higgs Bosons in Events with Multiple Bottom Quarks at the Tevatron*, `arXiv:1207.2757 [hep-ex]`.

[14] CDF Collaboration, T. Aaltonen et al., *Search for Higgs Bosons Produced in Association with b-quarks*, Phys.Rev. **D85** (2012) 032005, arXiv:1106.4782 [hep-ex].

[15] D0 Collaboration, V.M. Abazov et al., *Search for neutral Higgs bosons in the multi-b-jet topology in 5.2fb^{-1} of $p\bar{p}$ collisions at $\sqrt{s} = 1.96$ TeV*, Phys.Lett. **B698** (2011) 97–104, arXiv:1011.1931 [hep-ex].

[16] The CMS Collaboration, S. Chatrchyan et al., arXiv:1104.1619 [hep-ex] [hep-ex].

[17] The ATLAS Collaboration , *Search for the neutral Higgs bosons of the Minimal Supersymmetric Standard Model in pp collisions at $\sqrt{s} = 7$ TeV with the ATLAS detector*, arXiv:1211.6956 [hep-ex].

[18] T. A. Collaboration, *Observation of a new particle in the search for the Standard Model Higgs boson with the ATLAS detector at the LHC*, Physics Letters B **716** (2012) 1–29.

[19] T. C. Collatoration, *Observation of a new boson at a mass of 125 GeV with the CMS experiment at the LHC*, Physics Letters B **716** (2012) 30–61.

[20] S. Heinemeyer, O. Stål and G. Weiglein, *Interpreting the LHC Higgs search results in the MSSM*, Phys.Lett. **B710** (2012) 201–206, arXiv:1112.3026 [hep-ph].

[21] A. Arbey, M. Battaglia, A. Djouadi and F. Mahmoudi, *The Higgs sector of the phenomenological MSSM in the light of the Higgs boson discovery*, JHEP **1209** (2012) 107, arXiv:1207.1348 [hep-ph].

[22] The ATLAS Collaboration, G. Aad et al., *The ATLAS Experiment at the CERN Large Hadron Collider*, JINST **3** (2008) S08003.

[23] M. L. Mangano et al., *ALPGEN, a generator for hard multiparton processes in hadronic collisions*, JHEP **07** (2003) 001.

[24] J. Alwall et al., *Comparative study of various algorithms for the merging of parton showers and matrix elements in hadronic collisions*, Eur. Phys. J. **C53** (2008) 473, arXiv:0706.2569.

[25] S. Frixione and B. R. Webber, *Matching NLO QCD computations and parton shower simulations*, JHEP **06** (2002) 029, hep-ph/0204244.

[26] B. P. Kersevan and E. Richter-Was, *The Monte Carlo Event Generator AcerMC 2.0 with Interfaces to PYTHIA 6.2 and HERWIG 6.5*, `arXiv:0405247v1 [hep-ph]`.

[27] G. Corcella et al., *HERWIG 6: an event generator for hadron emission reactions with interfering gluons (including supersymmetric processes)*, JHEP **01** (2001) 010.

[28] J. M. Butterworth, J. R. Forshaw, and M. H. Seymour, *Multiparton Interactions in Photoproduction at HERA*, Z. Phys. **C72** (1996) 637.

[29] T. Binoth, M. Ciccolini, N. Kauer, and M. Kramer, *Gluon-induced W-boson pair production at the LHC*, JHEP **12** (2006) 046.

[30] A. S. et al., *Higgs boson production in gluon fusion*, JHEP **02** (2009) 029.

[31] T. Gleisberg et al., *Event generation with SHERPA 1.1*, JHEP **02** (2009) 007.

[32] J. Pumplin, D. R. Stump, J. Huston, H. L. Lai, P. M. Nadolsky and W. K. Tung, "New generation of parton distributions with uncertainties from global QCD analysis," JHEP **0207** (2002) 012 [hep-ph/0201195].

[33] H. -L. Lai, M. Guzzi, J. Huston, Z. Li, P. M. Nadolsky, J. Pumplin and C. -P. Yuan, "New parton distributions for collider physics," Phys. Rev. D **82** (2010) 074024 [arXiv:1007.2241 [hep-ph]].

[34] S. Heinemeyer *et al.* [LHC Higgs Cross Section Working Group Collaboration], "Handbook of LHC Higgs Cross Sections: 3. Higgs Properties," arXiv:1307.1347 [hep-ph].

[35] M. Carena, S. Heinemeyer, C. E. M. Wagner, and G. Weiglein, *Suggestions for benchmark scenarios for MSSM Higgs boson searches at hadron colliders*, Eur. Phys. J. **C26** (2003) 601–607, `hep-ph/0202167`.

[36] The ATLAS Collaboration, *ATLAS Monte Carlo Tunes for MC09*, ATL-PHYS-PUB-2010-002.

[37] S. Jadach, J. H. Kuhn and Z. Was, *TAUOLA - a library of Monte Carlo programs to simulate decays of polarized τ leptons*, Comput. Phys. Commun. **64** (1990) 275.

[38] E. Barberio, B. V. Eijk and Z. Was, *Photos - a universal Monte Carlo for QED radiative corrections in decays*, Comput. Phys. Commun. **66** (1991) 115.

[39] The GEANT4 Collaboration, S. Agostinelli et al., *GEANT4 - a simulation toolkit*, Nucl. Instrum. Meth. **A506** (2003) 250.

[40] The ATLAS Collaboration, G. Aad et al., *The ATLAS Simulation Infrastructure*, ATLAS-SOFT-2010-01-004, submitted to Eur. Phys. J. C., `arXiv:1005.4568`.

[41] The ATLAS Collaboration, *Estimation of $Z \to \tau\tau$ Background in VBF $H \to \tau\tau$ Searches from $Z \to \mu\mu$ Data using an Embedding Technique*, ATL-PHYS-INT-2009-109.

[42] The ATLAS Collaboration, *Search for the Standard Model Higgs boson in the $H \to \tau\tau$ decay mode with 4.7 f b1 of ATLAS detactor*, Tech. Rep. ATLAS-CONF-2012-014, CERN, Geneva, Mar, 2012.

[43] The ATLAS Collaboration, *Search for the Standard Model Higgs boson $H \to \tau\tau$ decays with the ATLAS detector*, ATL-COM-PHYS-2013-722.

[44] T. S. et al., Z *physics at LEP 1*, CERN 89-08 **3** (1989) 143.

[45] The ATLAS Collaboration, Inner Detector: Technical Design Report, CERN/LHCC/97-016/017 (1997).

[46] The ATLAS Collaboration, G. Aad et al., The ATLAS Experiment at the CERN Large Hardon Collider, 2008 JINST 3 S08003.

[47] A. Bazan, T. Bouedo, P. Ghez, M. Marino and C. Tull, "The Athena data dictionary and description language," eConf C **0303241** (2003) MOJT010 [cs/0305049 [cs-se]].

[48] The ATLAS Collaboration, *Expected Performance of the ATLAS Experiment - Detector, Trigger and Physics*, CERN-OPEN-2008-020, `arXiv:0901.0512`.

[49] T. Cornelissen et al., Concepts, Design and Implementation of the ATLAS New Tracking, ATLAS Note ATL-SOFT-PUB-2007-007 (2007).

[50] Kalman, R. E. (1960). *"A New Approach to Linear Filtering and Prediction Problems"*. Journal of Basic Engineering 82 (1): 3545. doi:10.1115/1.3662552

[51] The ATLAS Collaboration, Performance of primary vertex reconstruction in proton-proton collisions at $s = sqrt(7)$ TeV in the ATLAS experiment. ATLAS-CONF-2010-069.

[52] R. Fruhwirth, W. Waltenberger, P. Vanlaer, *Adaptive vertex fitting*, J. Phys. G34 (2007).

[53] The ATLAS Collaboration, *Characterization of Interaction-Point Beam Parameters Using the pp Event-Vertex Distribution Reconstructed in the ATLAS Detector at the LHC*, ATL-CONF-2010-027.

[54] The ATLAS collaboration, *Expected electron performance in the ATLAS experiment*, ATL-PHYS-PUB-2011-006

[55] The ATLAS Collaboration, *Electron reconstruction and identification efficiency measurements with the ATLAS detector using the 2011 LHC proton-proton collision data*, CERN-PH-EP-2014-040, arXiv:1404.2240

[56] The ATLAS Collaboration, G. Aad et al., *Electron performance measurements with the ATLAS detector using the 2010 LHC proton-proton collision data*, Eur.Phys.J. C72 (2012) 1909.

[57] S. Hassini, et al., *A muon identification and combined reconstruction procedure for the ATLAS detector at the LHC using the (MUONBOY, STACO, MuTag) reconstruction packages*, NIM A572 (2007) 7779.

[58] The ATLAS Collaboration, G. Aad et al., *Preliminary results on the muon reconstruction efficiency, momentum resolution, and momentum scale in ATLAS 2012 pp collision data*, ATLAS-CONF-2013-088, CERN, 2013,

[59] M. Cacciari, G. P. Salam, and G. Soyez, *FastJet user manual*, Eur.Phys.J. C72 (2012) 1896.

[60] W. Lampl et al., *Calorimeter Clustering Algorithms : Description and Performance*, ATL-LARG-PUB-2008-002.

[61] M. Cacciari, G. P. Salam, and G. Soyez, *The anti-kt jet clustering algorithm*, JHEP 04 (2008) 63.

[62] E. Abat, J. Abdallah, T. Addy, P. Adragna, et al., *Combined performance studies for electrons at the 2004 ATLAS combined test-beam*, JINST 5 (2010) P11006.

[63] ATLAS Collaboration, *Jet energy measurement with the ATLAS detector in proton-proton collisions at* $\sqrt{s} = 7$ *TeV*, Submitted to EPJ (2011) , arXiv:1112.6426

[64] The ATLAS Collaboration, *Pile-up corrections for jets from proton-proton collisions at ATLAS in 2011*, ATLAS-CONF-2012-064, July, 2012.

[65] M. Cacciari and G. P. Salam, *Pileup subtraction using jet areas*, Phys.Lett. B659 (2008) 119.

[66] The ATLAS Collaboration, G. Aad et al., *Jet energy resolution in proton-proton collisions at $\sqrt{s} = 7$ TeV recorded in 2010 with the ATLAS detector*, Eur.Phys.J. C73 (2013) 2306

[67] The ATLAS collaboration, *Jet energy scale and its systematic uncertainty in proton-proton collisions at $\sqrt{s} = 7$ TeV with ATLAS 2011 data*, ATLAS-CONF-2013-004

[68] The ATLAS Collaboration, *Data-Quality Requirements and Event Cleaning for Jets and Missing Transverse Energy Reconstruction with the ATLAS Detector in Proton-Proton Collisions at a Center-of-Mass Energy of $\sqrt{s} = 7$ TeV*, ATLAS-CONF-2010-038.

[69] G. Piacquadio, C. Weiser, *A new inclusive secondary vertex algorithm for b-jet tagging in ATLAS*, JPCS 119 (2008) 032032

[70] The ATLAS Collaboration, G. Aad et al., *Commissioning of the ATLAS high-performance b-tagging algorithms in the 7 TeV collision data, ATLAS-CONF-2011-102*, CERN, 2011, ATLAS-CONF-2011-102.

[71] The ATLAS Collaboration, *Measuring the b-tag efficiency in a ttbar sample with 4.7 fb^{-1} of data from the ATLAS detector* ATLAS-CONF-2012-097.

[72] The ATLAS Collaboration, *Calibration of b-tagging using dileptonic top pair events in a combinatorial likelihood approach with the ATLAS experiment* ATLAS-CONF-2014-004.

[73] The ATLAS Collaboration, *Reconstruction and Calibration of Missing Transverse Energy and Performance in Z and W events in ATLAS Proton-Proton Collisions at $\sqrt{s}$=7 TeV*, ATLAS-CONF-2011-080.

[74] ATLAS Collaboration, G. Aad et al., Performance of missing transverse momentum reconstruction in proton-proton collisions at 7 TeV with ATLAS, Eur.Phys.J. C72 (2012) 1844.

[75] TheATLAS Collaboration, *Performance of the Reconstruction and Identification of Hadronic tau Decays in ATLAS with 2011 Data*, ATLAS-CONF-2012-142.

[76] The ATLAS Collaboration, G. Aad et al., *Performance of the ATLAS trigger system in 2010*, Eur.Phys.J. C72 (2012) 1849.

[77] The ATLAS Collaboration, G. Aad et al., *Performance of the ATLAS muon trigger in 2011*, ATLAS-CONF-2012-099, CERN, 2012.

[78] The ATLAS Collaboration, G. Aad et al., *Performance of the ATLAS electron and photon trigger in p-p collisions at* $\sqrt{s} = 7$ *TeV in 2011*, ATLAS-CONF-2012-048, CERN, 2012.

[79] M. Dobbs and J.B. Hansen, *The HepMC C++ Monte Carlo Event Record for High Energy Physics*, Computer Physics Communications, ATL-SOFT-2000-001.

[80] A. Elagin, P. Murat, A. Pranko, and A. Safonov, *A New Mass Reconstruction Technique for Resonances Decaying to di-tau*, `arXiv:1012.4686 [hep-ex]`. * Temporary entry *.

[81] T. A. Collaboration, *Search for neutral MSSM Higgs bosons decaying to* $\tau\tau$ *pairs in proton-proton collisions at with the ATLAS detector*, Physics Letters B **705** (2011) no. 3, 174 – 192.

[82] The ATLAS Collaboration, *Data-driven estimation of the background to charged Higgs boson searches using hadronically-decaying tau final states in ATLAS,* ATLAS-CONF-2011-051.

[83] The ATLAS Collaboration, *Measurement of the* $Z \to \tau\tau$ *cross section with the ATLAS detector*, Phys. Rev. D **84** (2011) 112006.

[84] T. A. Collaboration, *Search for the neutral Higgs bosons of the Minimal Supersymmetric Standard Model in pp collisions at* $\sqrt{s} = 7$ *TeV with the ATLAS detector*, JHEP , `arXiv:1211.6956`.

[85] Atlas statistics forum, *ABCD method in searches*, link

[86] The ATLAS Collaboration, *Search for Neutral MSSM Higgs Bosons H to* $\tau\tau$ *to* $l\tau_h$ *with the ATLAS Detector in 7 TeV Collisions*, ATL-COM-PHYS-2012-094.

[87] The ATLAS Collaboration, *Search for neutral Higgs Bosons in the decay mode* $H \to \tau\tau \to ll{+}4\nu$ *in proton proton collision at* $\sqrt{7}$ *TeV with the ATLAS Detector*, ATL-COM-PHYS-2011-758.

[88] The ATLAS Collaboration, *Luminosity Determination in pp Collisions at* $\sqrt{s} = 7$ *TeV using the ATLAS Detector in 2011*, ATLAS-CONF-2011-116.

[89] T. Sjostrand, S. Mrenna and P. Skands, *PYTHIA 6.4 physics and manual*, JHEP **05** (2006) 026.

[90] A. B. et al., *Rivet user manual*, arXiv:1003.0694 [hep-ph].

[91] E. G. G. Cowan, K. Cranmer and O. Vitells, *Asymptotic formulae for likelihood-based tests of new physics*, arXiv:1007.1727 [hep-ex].

[92] LHC Higgs Cross Section Working Group, S. Dittmaier, C. Mariotti, G. Passarino, R. Tanaka (Eds.), et al., *Handbook of LHC Higgs Cross Sections: 1. Inclusive Observables*, arXiv:1101.0593 [hep-ph].

[93] LHC Higgs Cross Section Working Group, S. Dittmaier, C. Mariotti, G. Passarino, and R. Tanaka (Eds.), *Handbook of LHC Higgs Cross Sections: 2. Differential Distributions*, CERN-2012-002 (CERN, Geneva, 2012) , arXiv:1201.3084 [hep-ph].

[94] ATLAS collaboration *Performance of the ATLAS Silicon Pattern Recognition Algorithm in Data and Simulation at* $\sqrt{s} = 7$ *TeV*, ATLAS-CONF-2010-072

[95] The ATLAS Collaboration, *A measurement of the material in the ATLAS inner detector using secondary hadronic interactions*, arXiv:1110.6191, JINST 7 (2012) P01013

[96] The ATLAS Collaboration, *Validation of the ATLAS jet energy scale uncertainties using tracks in proton-proton collision* $\sqrt{s} = 7$ *TeV*, ATLAS-CONF-2011-067

[97] The ATLAS Collaboration, *Track Reconstruction Efficiency in* $\sqrt{s} = 7$ *TeV Data for Tracks with* $P_T > 100$ *MeV* , ATL-PHYS-INT-2010-112

[98] D. de Florian, G. Ferrera, M. Grazzini and D. Tommasini, *Transverse-momentum resummation: Higgs boson production at the Tevatron and the LHC*, JHEP **1111** (2011) , arXiv:1109.2109 [hep-ph].

[99] Statistical twiki, NuissanceCheck. https://twiki.cern.ch/twiki/bin/view/AtlasProtected/Nuisan